

Detection and Symbol Synchronization for Multiple-Bit per Photon Optical Communications

W. K. Marshall

Communications Systems Research Section

Methods of detection and synchronization in a highly efficient direct detection optical communication system are reported. Results of measurements on this moderate-rate demonstration system capable of transmitting 2.5 bits/detected photon in low-background situations indicate that symbol slot synchronization is not a problem, and that a simple symbol detection scheme is adequate for this situation. This system is a candidate for interplanetary optical communications.

I. Introduction

In a *signal limited* optical communication system, the data rate is determined by the number of received photons per second and the amount of data which can be communicated per received photon. The number of bits per received photon is a figure of merit of the efficiency of a given system and depends, in general, on the method of communications and on the quality of the receiver.

In a *photon counting* communication system information is sent by on-off modulating of a laser, with the laser output constant over a basic time interval called a *symbol slot*. The receiver estimates whether the laser was on or off during each symbol slot by counting the number of photon arrivals during that slot. A photon arrival is the result of extracting one quantum of energy (a photon) from the optical field incident on a detector to produce a photoelectron. The rate at which photoelectrons are generated is proportional to the incident optical intensity, but the actual number of photoelectrons is a random variable. A photon counting receiver has two tasks, symbol detection (estimating from the electrical output of the photon

counter whether the laser was on or off during a slot) and synchronization (determining the time position of symbol slots over which to count photons).

An efficient method of communicating with direct detection is to use M -ary pulse position modulation (PPM) (Ref. 1), in which the position of one *signal slot* (symbol slot in which the laser was “on”) among $M - 1$ *noise slots* (symbol slots in which the laser was “off”) in a PPM word represents $\log_2 M$ bits of information. In this article, the receiver section for a photon counting optical communication system which uses an average of less than 3 photon arrivals per signal slot with 256-ary PPM to achieve an efficiency of 2.5 bits/detected photon¹ is reported. The system communicates reliably (using Reed-Solomon error correction coding) at 300 kbps in low-background light situations.

¹Detected photons are different from *received* photons since the quantum efficiency of the photon counter is less than one. We use bits/detected photon to avoid the wavelength dependence of the efficiency of the photon counter (typically a PMT).

In the first section below, the *symbol detector* which detects photon arrivals and assigns them to appropriate time slots is described. The following section discusses the performance of this detector and its use in calibrating the system at the very low optical signal levels used (typically less than 1 picowatt). The next section considers the slot synchronizer and its performance. Note that this report presents experimental results on the receiver section of a fully operational 2.5 bit/detected photon demonstration system; reports on other aspects of this system are listed in Refs. 2-4.

II. Symbol Detection

The direct-detection receiver used in the 2.5 bit/detected photon demonstration program consists of a symbol detector and a phase-locked-loop slot synchronizer (Fig. 1). A photomultiplier tube (PMT) converts each photon arrival into a relatively large but random current pulse which drives the receiver. The symbol detector converts the (amplified) electrical output of the PMT into a signal indicating the reception of photons during time intervals (slots) determined by the slot synchronizer. The output of the detector is ultimately used by the PPM decoder to determine which of the M possible words (for M -ary PPM) was sent during each group of symbols which make up a PPM word.

In general, the problem of estimating photon arrivals from the electrical output of the PMT is quite difficult. For optimal PPM demodulation, the detector should be able to determine the number of photon arrivals during each of the symbol slots in a PPM word. Because of random PMT gain (i.e., PMT output pulses have variable height and width; Ref. 5), thermal noise in the amplified PMT output and limited time resolution (due to limited bandwidth), the estimation problem becomes quite difficult. However, in cases in which the channel is erasure-limited, (i.e., the probability of a background photon arrival during a PPM word is less than the probability that no signal photons are received due to the Poisson statistics of photon arrivals), the detection problem reduces to classifying slots only according to whether there were no photon arrivals (symbol detected as "0") or some photon arrivals (symbol detected as "1") during each slot. For the 2.5 bit/detected photon demonstration this erasure-limited condition is satisfied for background levels up to about 2000 noise counts/s (footnote 2); hence, the detector used here classifies slots only according to some photon arrivals or none.

The symbol detector used for these experiments is very simple and consists of a voltage threshold comparator and a

latch. If the (amplified 700X) output of the PMT crosses the voltage threshold during a symbol slot marked by rising edges on the estimated slot clock input, the latch output is "1" and a photon is declared to have arrived during that slot. Since the average height of the PMT pulses is much higher than the rms thermal noise voltage, almost all of the threshold crossings indicate photon arrivals. As shown in this next section, this detector circuit, although simple, performs satisfactorily in the few photons per signal slot regime.

III. Detector Performance

In order to measure the performance of the detector independent of synchronization errors, the clock was initially hard-wired from the transmitter (with appropriate delays). The fraction of signal slots in which photons were detected (i.e., voltage threshold crossed) as a function of the detector threshold for three different signal intensities is shown in Fig. 2. The probability of detecting at least one photon during a signal slot, P_{ds} , is approximately constant over a wide range of thresholds (40-200 mV at the comparator input) but falls off quite rapidly at higher thresholds. The probability of detection in this constant P_{ds} region depends on the intensity in a way related to the Poisson distribution of the number of photon arrivals. In slots during which the laser is turned off (and the background intensity is essentially zero), there is still some probability that the threshold will be crossed due to thermal noise and due to the presence of PMT dark counts. The fraction of noise slots, $(1 - P_{dn})$, in which the threshold was crossed with no optical signal is shown in Fig. 3. This graph shows two distinct regions of operation. For $V_{\text{thresh}} < \sim 50$ mV, $(1 - P_{dn})$ decreases rapidly as the threshold is increased, due to the decreased probability that thermal noise will cause a threshold crossing. Above 50 mV, the fraction of false counts is almost constant at about 2×10^{-6} . This is the result of PMT dark counts which for the cooled RCA C31034 PMT used were about 20 per second.

The approximate shape of the P_{ds} versus threshold voltage curve can be predicted using the simple theory that a given photoelectron response pulse is detected if the (random) PMT gain seen by the pulse is greater than a gain threshold given by $G_{\text{thresh}} = (V_{\text{thresh}}/700) T_{\text{pulse}}/R_{\text{term}}$ (electrons), where T_{pulse} is the (average) width of the amplified PMT single photoelectron response pulses and R_{term} is the PMT termination resistance. The probability of detecting a given single photoelectron response pulse is the probability that the gain is greater than G_{thresh} , given by

$$P(\text{Gain} > G_{\text{thresh}}) = \int_{G_{\text{thresh}}}^{\infty} p_G(x) dx \quad (1)$$

²For comparison, a diffraction-limited receiving telescope looking at Jupiter from Earth-orbit through a 10 angstrom filter at $0.9 \mu\text{m}$ would produce 10^3 to 10^4 detected background photons per second.

where $p_G(x)$ is the probability density of the PMT gain given approximately (Ref. 6) by

$$p_G(x) = \exp(-A/B) (\delta(x) + \frac{\exp(-x/B) \sqrt{A/x}}{B} I_1((2/B) \sqrt{A x})) \quad (2)$$

where for the PMT used, $A = 10^6$ (the mean PMT gain) and $B = 1.42 \times 10^5$, and I_1 is the modified Bessel function of the first kind. The overall P_{ds} is the probability of detecting a pulse containing a given number of photoelectron pulses averaged over the (Poisson) distribution of the number of photon arrivals in a signal slot. This curve is given in Fig. 4 and matches the experimental curve reasonably well for thresholds large enough to ignore thermal noise. The theory curve shows that for thresholds less than about 0.2 times the mean value, the detector should be nearly ideal, limited only by the Poisson photon erasure statistics, i.e.,

$$P_{ds} \cong 1 - \exp(-N_s) \quad (3)$$

where N_s is the mean number of photon arrivals per signal slot. Hence for a voltage threshold of 70 mV (used for measurements throughout the remainder of this report) the signal intensity, N_s , is given by

$$N_s \cong -\ln(1 - P_{ds}(70 \text{ mV})) \quad (4)$$

By using an additional photodetector to measure the laser output before it was attenuated (by ~ 80 dB) and fed into the PMT, the value of N_s corresponding to various transmitter pulse widths and monitor photodiode voltages was measured (Fig. 5) and used to calibrate the received signal intensity. Note that the intensities given relate to the number of photoelectrons generated during a signal slot, and are therefore related to the actual (peak) optical intensity by the PMT quantum efficiency, η_{QE} , the energy per photon, $h\nu$, and the slot width, T , by

$$\text{Optical power} = \frac{N_s h\nu}{\eta_{QE} f T} \quad (5)$$

where f is the fraction of a symbol slot filled by a laser pulse. For a wavelength of $0.85 \mu\text{m}$, $h\nu = 2.3 \times 10^{-19}$ Joule, and $\eta_{QE} = 0.2$, $f = 0.7$, and $T = 100$ ns, the *peak* optical power incident on the PMT photocathode is

$$\text{Optical power} \cong 2 N_s \times 10^{-11} \text{ Watts} \quad (6)$$

For 256-ary PPM and $N_s = 3$, the *average* incident optical power would be ~ 0.25 picowatts.

IV. Symbol Slot Synchronization

Symbol slot synchronization in the direct-detection receiver is the reconstruction of the transmitter clock rate and phase to determine the intervals over which to count photon arrivals. The receiver must track the transmitter clock, using relatively few discrete photon arrivals (with random arrival times), where the primary noise sources are signal photon shot noise, shot noise due to background photons, and noise due to PMT gain fluctuations. Initial (linear) calculations for this case indicated that a PLL tracking loop would work, provided the loop bandwidth was sufficiently small. A symbol slot synchronizer using this approach was designed and constructed and operated with satisfactory results as discussed below.

The slot synchronizer portion of the receiver consists of a phase detector, an active low-pass filter and a precision voltage-controlled oscillator (VCO). The input to the loop is from the voltage comparator in the symbol detector, a binary signal which is "1" whenever the PMT output is above the voltage threshold. This signal is gated with the VCO output clock in the phase detector and filtered to produce the error input to the VCO.

The closed loop response of the PLL is (approximately)

$$H(s) = K(1 + s T_2)/(s^2 T_1 + K(1 + s T_2)) \quad (7)$$

where $K = (K_\phi K_{VCO})$ is the combined gain of the phase detector and the VCO, and $T_1 = (R_1 C_2)$, $T_2 = (R_2 C_2)$ are the loop filter time constants. The phase detector gain K_ϕ is a function of the signal level N_s and the fraction of slots during which the laser is on ($= 1/M$ for M -ary PPM). Although K_ϕ is actually a non-linear function of the signal level, for small N_s it can be (empirically) approximated by

$$K_{\phi} \cong 0.06 \frac{N_s}{M} \text{ volts/radian} \quad (8)$$

The VCO gain was

$$K_{VCO} = 750 \text{ radians/sec/volt} \quad (9)$$

so that the combined gain was

$$K \cong 50 \frac{N_s}{M} \text{ sec}^{-1} \quad (10)$$

By an extension of the results in Ref. 7, the steady-state rms timing error due to shot noise is given approximately by

$$\frac{T_{\text{rms}}}{T} = f \sqrt{\frac{B(N_s) M T}{2 N_s} \left(1 + \frac{N_b M}{N_s}\right)} \quad (11)$$

where $B(N_s)$ is the one-sided loop noise bandwidth, M is the number of symbols in a PPM word, and N_b is the mean number of photon arrivals per noise slot. For the transfer function $H(s)$ given in Eq. (7) and the gain given by Eq. (10), the noise bandwidth is given (Ref. 8) by

$$B(N_s) = B_1 + B_2 N_s \quad (12)$$

where $B_1 = 1/(4 T_2)$ and $B_2 = (50/M) T_2/(4 T_1)$, so that the expected rms timing error is given by

$$\frac{T_{\text{rms}}}{T} = f \sqrt{\frac{M T}{2} \left(\frac{B_1}{N_s} + B_2 \right) \left(1 + \frac{N_b M}{N_s} \right)} \quad (13)$$

Measured values of T_{rms} versus signal level are shown for three different loop filters in Fig. 6, for four pulse width fractions in Fig. 7, and for three values of N_b in Fig. 8. Symbol tracking down to better than 1/50 of a symbol slot (i.e., < 2 ns) was achieved using an appropriately narrow loop ($B_1 = 16/\text{sec}$, $B_2 = 6/\text{sec}$). The results show the expected dependence on loop bandwidth, pulse width, and background intensity, but the actual values of T_{rms}/T were two to four times greater than predicted by Eq. (10). Likely sources of error are inaccuracies in estimating the phase detector gain K_ϕ and the loop filter response to pulsed input.

Acquisition performance of the demonstration system was determined experimentally, although there are no theoretical results to compare them with. Since the loop idled at the

upper frequency limit, unaided acquisition required that the loop pull-in from the VCO limit of 1 kHz above the slot frequency of 10 MHz. This occurred for loop filter 1 (as listed in Fig. 6) almost instantaneously (fractions of a second), but not for the other filters which produced narrower loops. However, by pulling the VCO down to -1 kHz and letting it drift upward towards the center frequency (simulating swept acquisition), all the filters used produced reliable acquisition.

V. Conclusions

The intent in constructing the receiver described in this article and the rest of the 2.5 bit/detected photon system was to demonstrate that the concepts of multiple bit per photon direct detection communications were valid, and to show that a practical system could be built. This goal was successfully accomplished.

The 300 kbps rate of the system was chosen to outperform existing deep space links which use microwaves; a factor of 10 improvement in rate could be made by employing faster electronics, but at a cost of higher average laser power (since the number of bits/photon is constant). Alternatively, faster electronics in the receiver only would allow the symbol detector to run at 10 times the slot rate. This would allow the PPM demodulator to make soft decisions (based on the number of sub-symbols in which photons were counted) to determine which PPM word was sent, resulting in substantial improvement of the system's performance in higher background light situations.

References

1. J. R. Pierce, Optical channels: practical limits with photon counting, *IEEE Trans. Commun. COM-26*, pp. 1819-1821, Dec. 1978.
2. J. R. Lesh, Optical communications research to demonstrate 2.5 bits/detected photon, *IEEE Communications Magazine* 20, No. 6, pp. 35-37, Nov. 1982.
3. J. Katz, 2.5 bit/detected photon demonstration program: Phase II and III experimental results, *TDA Progress Report 42-70*, pp. 95-104, Jet Propulsion Laboratory, California (1982).
4. W. K. Marshall, A PPM modulator and demodulator for the 2.5 bit/detected photon demonstration, *TDA Progress Report 42-68*, pp. 50-54, Jet Propulsion Laboratory, California (1982).
5. R. W. Engstrom, *RCA Photomultiplier Handbook PMT-62*, Ch. 4, RCA Solid State Division, Lancaster, PA, 1980.
6. H. H. Tan, A statistical model of the photomultiplier gain process with applications to optical pulse detection, *TDA Progress Report 42-68*, pp. 55-67, Jet Propulsion Laboratory, Pasadena, CA, 1982.
7. V. A. Vilnrotter, et al., A synchronization technique for optical PPM signals, submitted to *IEEE Transactions on Communications*.
8. W. C. Lindsey, *Synchronization Systems in Communications and Control*, Ch. 4, Prentice-Hall, Englewood Cliffs, NJ, 1972.

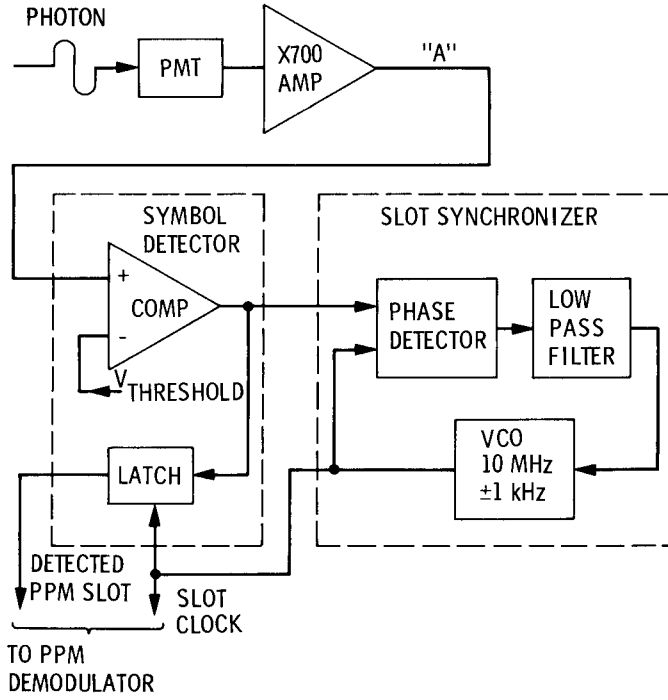


Fig. 1. Direct-detection receiver

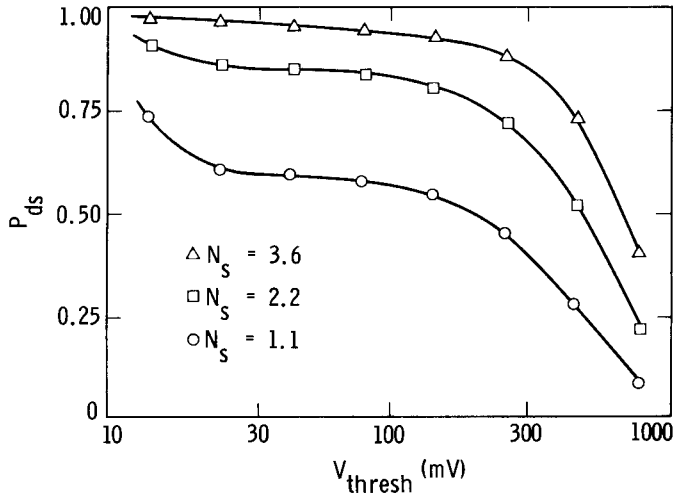


Fig. 2. Relative frequency of detected symbol "1" during signal slots, P_{ds} , vs threshold voltage, V_{thresh} (mV)

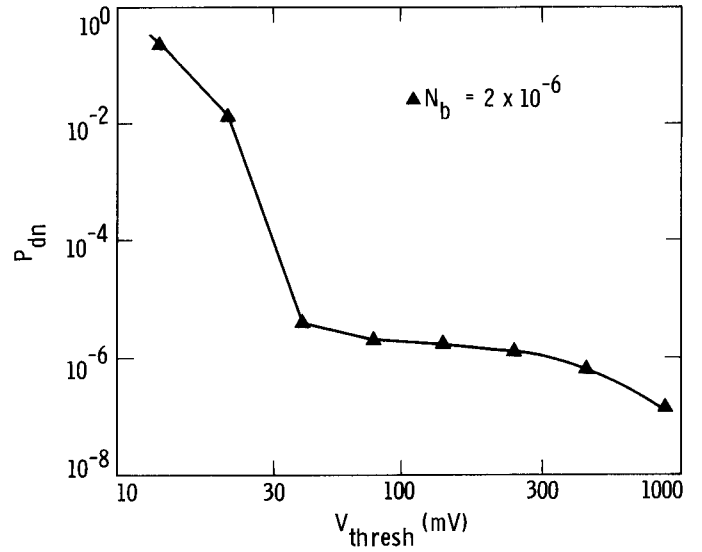


Fig. 3. Relative frequency of detected symbol "1" during noise slots ($1 - P_{dn}$) vs threshold voltage, V_{thresh} (mV)

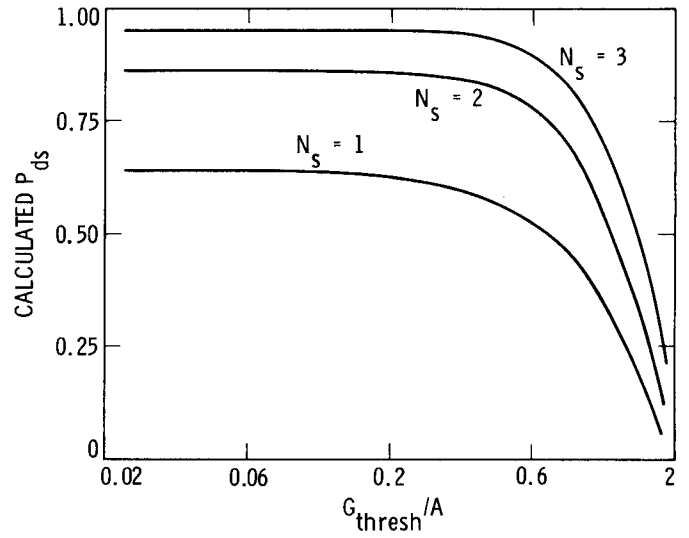


Fig. 4. Calculated P_{ds} vs normalized gain threshold, (G_{thresh}/A)

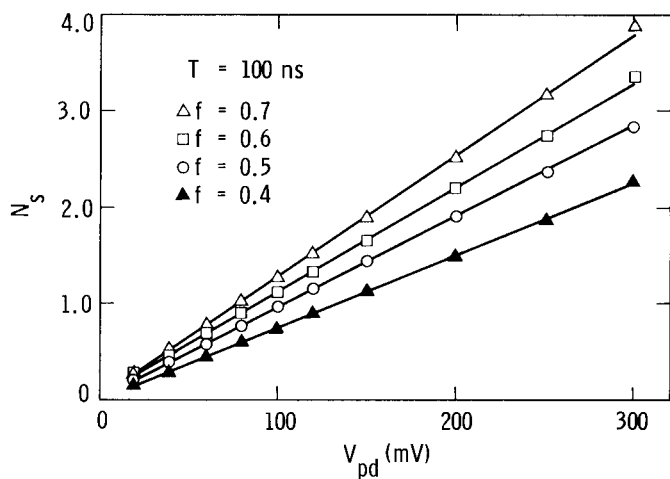


Fig. 5. Detected photons per signal slot, N_s , vs monitor photodiode voltage, V_{pd} (mV)

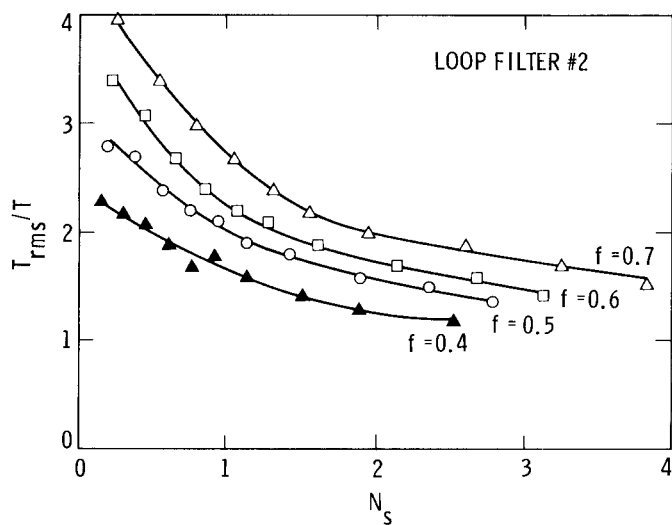


Fig. 7. T_{rms}/T vs N_s for different laser pulse width fractions, f

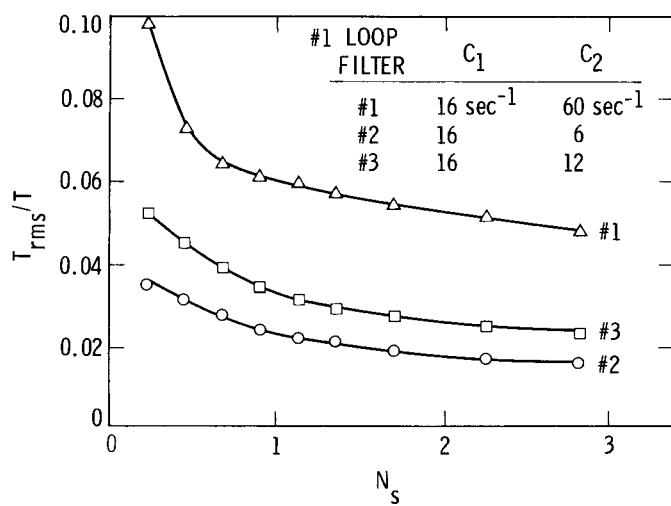


Fig. 6. T_{rms}/T vs N_s for $f = 0.6$ and various loop filters

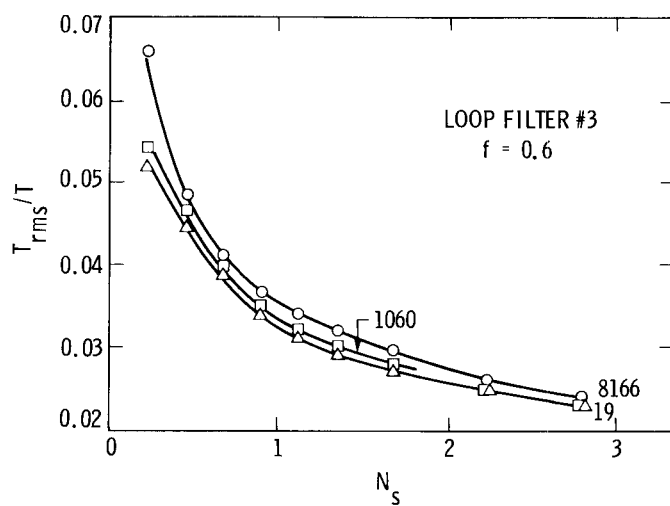


Fig. 8. T_{rms}/T vs N_s for different background levels, N_b